Isolated delayed metastasis to the talus from Ewing's sarcoma

Layla Nasr[1], Lena Naffaa[1*], Alaeddine El Alayli[1], Miguel R Abboud[2], Nabil J Khoury[1]

1. Department Of Radiology, American University Of Beirut Medical Center, Beirut, Lebanon

2. Department of Pediatrics and Adolescent Medicine, American University of Beirut Medical Center, Beirut, Lebanon

* **Correspondence:** Lena Naffaa, MD, Department Of Radiology, American University Of Beirut Medical Center, P.O.Box 11-0236, Beirut, Lebanon
(*ln01@aub.edu.lb*)

Radiology Case. 2018 Aug; 12(8):17-24 :: DOI: 10.3941/jrcr.v12i8.3164

ABSTRACT

Bone metastasis to the hands and feet, known as acrometastasis, is a very rare finding and tends to be associated with extensive metastasis. We herein report the case of a 14-year-old girl known to have a history of successfully treated Ewing's sarcoma arising from the ribs, who presented with a pathologically proven isolated metastatic lesion to the talus 7 years after achieving clinical and radiologic remission. We describe the imaging findings on MRI, CT scan and PET-CT. To our knowledge, talar metastasis from Ewing's sarcoma has been previously reported only twice in the English literature. Noteworthy is the fact that one of the previously reported lesions was considered a skip metastasis, and the other was under-described in terms of primary and secondary tumor location and time to metastasis. In addition, the overall imaging findings were rather suggestive of a benign lesion, particularly on CT scan.

Journal of Radiology Case Reports

www.RadiologyCases.com

CASE REPORT

CASE REPORT

The patient is a 14-year-old girl who was diagnosed with a large chest wall Ewing's sarcoma (ES) arising from the right 6th rib at the age of 7 years. Workup for metastatic disease using bone scans, PET-CT scans, and CT scans of the chest and abdomen was initially negative and throughout treatment as well (Figure 1). She received chemotherapy consisting of vincristine, doxorubicin and cyclophosphamide (VDC) alternating every two weeks with ifosfamide and etoposide (IE) a per the CCG 7942 protocol. At the time of local control, she was found to have complete response with no evidence of residual disease. She nonetheless received radiation therapy to the right hemithorax as needle biopsy of the tumor had been complicated by hemorrhage. Periodic follow-up with enhanced CT scans of the chest and abdomen, chest MR imaging, and bone scans confirmed that she remained disease-free throughout 7 years after end of therapy.

The patient currently presented with a 2-week history of left ankle pain of insidious onset, without swelling or erythema, and with no other associated systemic symptoms. There was no history of trauma or other precipitating factors.

On physical exam, she had mild tenderness at the anterolateral aspect of ankle and sinus tarsi, with limited motion of the subtalar joint due to pain.

In view of the patient's history, an MRI of the ankle and foot was ordered as initial imaging study and it showed a lesion at the head and neck of the talus (Figure 2A-C). This was of low signal intensity on T1-weighted images (Figure 2A), heterogeneously high signal on short-tau inversion-recovery (STIR) sequence (Figure 2B), and showed heterogeneous enhancement following gadolinium IV contrast injection (Figure 2C). There was mild enhancing edema in the surrounding bone marrow and soft tissues, mainly at the sinus tarsi. Focal cortical disruption was present.

Non-enhanced CT scan was then obtained (Figure 3A-B) and showed a well-defined lytic lesion with thick trabeculae and a sclerotic rim. The differential diagnosis prior to the biopsy results included chondroblastoma, partially healed bone cyst or aneurysmal bone cyst, giant cell tumour, and a low likelihood of metastasis. Focal cortical disruption was present (Figure 3A).

CT-guided core biopsy of the talar lesion was then performed showing marrow spaces invaded by neoplastic cells, most of which appeared necrotic with an undifferentiated phenotype and uniform cytology (Figure 4A).

Immunohistochemical markers were positive for vimentin and CD99 (Figure 4B). Overall findings were typical of ES. Whole body PET/CT with 18-Fluoro-deoxyglucose (FDG) for metastatic workup was then performed and showed increased radiotracer uptake at the level of the talar lesion with a mean standardized uptake value (SUV) of 1.72 and maximal SUV of 2.4 (Figure 5). However, there was no evidence of active disease elsewhere in the body.

The patient then underwent a chemotherapy treatment followed by a rescue autologous hematopoietic stem cell transplant with radiation therapy.

Follow up PET-CT and MRI demonstrated residual abnormal signal which decreased over time then stabilized suggesting post treatment changes.

DISCUSSION

Etiology & Demographics:

Bone metastasis to the hands and feet, known as acrometastasis is a rare finding, usually occurring in patients with extensive metastatic disease, and is believed to be underdiagnosed. However, it has been reported as the initial presentation of occult malignancies (1). The hands are more frequently involved than the feet(1), and the calcaneus is the single most frequently involved bone in the foot, followed by the talus (1-3). The most common single organs from which malignancies metastasize to the foot are the lungs, kidneys, colon, and breasts (1-3).

It is estimated that 20% to 30% of patients with malignancy will develop skeletal metastasis in the course of their disease. However, the incidence of foot and ankle metastasis among all cancer patients is on average 0.01% with an estimated range of 0.007% to 0.3% (1). The relatively lower blood supply to the distal lower extremity is thought to be responsible for this low incidence, since bone metastasis usually occurs via hematogenous route (4).

Ewing's sarcoma most commonly affects the diaphysis of long bones; more than 50% of cases occur in the 10 to 20-year-old age group (5). It is a highly metastatic malignancy (6). The most common sites for metastasis are the lungs, followed by the bones (7). However, to our knowledge, metastasis to the bones of the foot from ES has only been reported twice in the English literature; the first case was mentioned in a review by Bakotic et al (3) with no mention of the primary's location, the specific affected tarsal bone, or the time lapse between primary diagnosis and metastasis occurrence. The second was by Jalal et al (8), where the talus was involved at the time of diagnosis by a skip lesion from a primary ES of the calcaneus. This is in contrast to primary ES, where 3% of lesions arise from the foot (1) with the talus being one of the least commonly involved bones (5, 9).

Clinical & Imaging findings:

Radiologically, Ewing's sarcoma of bone appears as a permeative lesion with aggressive periosteal reaction (onion skinning) and usually large soft tissue component (10). However, it is estimated that around half of ES arising in the talar bones have an atypical, non-specific appearance that can even mimic benign lesions with a differential that includes benign tumors and osteomyelitis (5). Such was the case with our patient, where our presumptive CT diagnosis was primarily chondroblastoma despite focal cortical disruption (Figure 4A).

On MRI, Ewing sarcomas display bone marrow replacement, cortical destruction and a soft tissue mass (10). On MR T1-weighted images, the signal is intermediate; on T2-weighted images, the signal is low-intermediate (10). In the case of Jalal et al., the talar metastasis of ES had a hypointense signal on T1- and T2-weighted images and displayed peripheral enhancement after gadolinium administration (8).

In our patient, the tumor appeared more aggressive on MR imaging than on CT scan, showing heterogeneous enhancement and surrounding bone marrow and soft tissue edema. However, chondroblastoma was still highly considered since such aggressive MR features have been also described in this benign tumor and since acrometastasis is extremely rare.

At present, the imaging modality of choice for the evaluation for disease recurrence in ES is FDG-PET/CT scan (7). The mean SUV for intra-osseous ES is estimated to be 5.3, compared to the mean SUV of all malignant bone lesions which is at 4.34 (11). However, PET/CT results may be operator-dependent and no large trials exist to confirm such values (11). Thus, even though our patient's lesion had a low mean SUV of 1.72 (Figure 4), it was confirmed to be an ES metastatic deposit.

Since 7 years elapsed during which PET-CTs and Bone Scans were repetitively normal, the possibility of our patient's tumor representing a metachronous lesion is unlikely.

Treatment & Prognosis:

Ewing's sarcoma treatment, while still debatable, typically consists of neoadjuvant chemotherapy in conjunction with surgery and/or radiation therapy followed by consolidation adjuvant chemotherapy. The first-line treatment is the same as the one presented in our case, i.e. a combination of vincristine, doxorubicin, and cyclophosphamide alternating with ifosfamide and etoposide, since our patient did not have metastases at initial diagnosis (2). Assessment of local control is done via imaging or pathological evaluation of tumor viability. Patients with no to minimal response can be switched

Journal of Radiology Case Reports
www.RadiologyCases.com

to one of the various second-line protocols (2, 12). Following neoadjuvant treatment, radiation therapy was traditionally the preferred method of local control. In recent years, with improvement of surgical technique, there has been a tendency toward surgical removal of the tumor instead of radiotherapy with no solid evidence comparing the outcomes of either approach (12).

However, metastatic recurrent disease away from the primary tumor represents a therapeutic challenge. Five-year survival of patients with localized disease (~80%) is significantly higher than those with pulmonary disease (~40-30%); osseous metastasis portends an even worse prognosis (~30-19% five-year survival) (12, 13). Treatment of recurrent disease is variable and controversial. Isolated distant bone recurrence is treated with a camptothecin-based regimen of chemotherapy (irinotecan/temozolomide or topotecan/cyclophosphamide) and local control (surgery and/or radiation) with increased overall and event-free survival (14-17). Many experimental new agents targeting the EWS-ETS fusion product and its signaling cascade are under trial for recurrent ES (18).

Differential Diagnoses:

When present, acrometastasis to the foot manifests as pain with or without erythema, swelling, and warmth, thus mimicking a wide range of pathologies which includes mainly monoarticular arthritides, infectious, traumatic, and other neoplastic processes (1). Therefore, it is essential to correlate radiologic and pathologic findings with the patient's previous history to reach a definitive diagnosis.

After obtaining MRI and CT scans of the patient, the following differential diagnosis was proposed.

Chondroblastoma

These benign tumors are uncommon and present in the first two decades of life (19, 20). The radiological features of chondroblastoma are similar to our case. On CT scan they are lucent lesions that show marked cortical destruction and periosteal reaction (20, 21). A lacelike matrix mineralization is also commonly present on CT (20, 21). On T1-weighted imaging, the lesion has low to intermediate signal; on T2-weighted and short-tau-inversion recovery (STIR) imaging, they have intermediate to high signal (21). These tumors can have aggressive features and surrounding soft tissue edema on MRI (21). The FDG uptake of these lesions is high (tumor-to-background ratio = 6.5 - 33.6), (SUVmax usually >2.5) (22).

Giant cell tumor

Comprising 15-20% of all benign bone tumors, these lesions typically occur in the third to fourth decades of life (19). On CT scan they are lytic lesions with potentially aggressive pattern of cortical destruction (19, 23). On MR imaging, these lesions have fluid-like signal intensity appearing low to intermediate on T1-weighted and high signal on fluid sensitive sequences (19, 22-24) with areas of enhancement after gadolinium contrast medium administration (24). Giant cell tumors also have increased uptake on PET scan (SUV > 2.0) (19, 22).

Aneurysmal bone cyst

Common in the first two decades of life, aneurysmal bone cysts (ABCs) are radiolucent lesions that most commonly occur in the metaphysis of long bones (19, 25). These lesions can expand over time and develop a thin outer rim with destruction of adjacent bone and a periosteal reaction (19, 25). A fluid-fluid level, best seen on MRI, is common (19, 25). T1- and T2-weighted signals are variable due to the variable composition of the cyst. ABCs can arise from preexisting bone tumors such as the two previously mentioned tumors (chondroblastoma and giant cell tumors).

TEACHING POINT

Acrometastasis from Ewing's Sarcoma is rare and can present with non-specific clinical signs and symptoms mimicking a benign or malignant process. the imaging findings on CT scan, MRI and PET-CT are not characteristic. Acrometastasis should always be on the differential diagnosis in light of history of malignancy and is confirmed by PET-CT and histopathology.

REFERENCES

1. Maheshwari AV, Chiappetta G, Kugler CD, Pitcher JD, Jr., Temple HT. Metastatic skeletal disease of the foot: case reports and literature review. Foot Ankle Int. 2008;29(7):699-710. PubMed PMID: 18785420.

2. Granowetter L, Womer R, Devidas M, Krailo M, Wang C, Bernstein M, et al. Dose-intensified compared with standard chemotherapy for nonmetastatic Ewing sarcoma family of tumors: a Children's Oncology Group Study. J Clin Oncol. 2009;27(15):2536-41. PubMed PMID: 19349548

3. Bakotic B, Huvos AG. Tumors of the bones of the feet: the clinicopathologic features of 150 cases. J Foot Ankle Surg. 2001;40(5):277-86. PubMed PMID: 11686448.

4. Rybak LD, Rosenthal DI. Radiological imaging for the diagnosis of bone metastases. Q J Nucl Med. 2001;45(1):53-64. PubMed PMID: 11456376.

5. Baraga JJ, Amrami KK, Swee RG, Wold L, Unni KK. Radiographic features of Ewing's sarcoma of the bones of the hands and feet. Skeletal Radiol. 2001;30(3):121-6. PubMed PMID: 11357448.

6. Hatano M, Matsumoto Y, Fukushi J, Matsunobu T, Endo M, Okada S, et al. Cadherin-11 regulates the metastasis of Ewing sarcoma cells to bone. Clin Exp Metastasis. 2015;32(6):579-91. PubMed PMID: 26092671.

7. Moore DD, Haydon RC. Ewing's sarcoma of bone. Cancer Treat Res. 2014;162:93-115. doi: 10.1007/978-3-319-07323-1_5. PubMed PMID: 25070232.

Journal of Radiology Case Reports

www.RadiologyCases.com

8. Jalal H, Belhadj Z, Enneddam H, Madhar M, Fikry T, Essadki O, et al. Contribution of magnetic resonance imaging in the diagnosis of talus skip metastases of Ewing's sarcoma of the calcaneus in a child: a case report. J Med Case Rep. 2011;5:451. PubMed PMID: 21910875.

9. Casadei R, Magnani M, Biagini R, Mercuri M. Prognostic factors in Ewing's sarcoma of the foot. Clin Orthop Relat Res. 2004(420):230-8. PubMed PMID: 15057103.

10. Murphey MD, Senchak LT, Mambalam PK, Logie CI, Klassen-Fischer MK, Kransdorf MJ. From the radiologic pathology archives: ewing sarcoma family of tumors: radiologic-pathologic correlation. Radiographics. 2013;33(3):803-31. PubMed PMID: 23674776.

11. Bestic JM, Peterson JJ, Bancroft LW. Pediatric FDG PET/CT: Physiologic uptake, normal variants, and benign conditions [corrected]. Radiographics. 2009;29(5):1487-500. PubMed PMID: 19755607.

12. Subbiah V, Anderson P, Lazar AJ, Burdett E, Raymond K, Ludwig JA. Ewing's sarcoma: standard and experimental treatment options. Curr Treat Options Oncol. 2009;10(1-2):126-40. PubMed PMID: 19533369.

13. Friedman DN, Chastain K, Chou JF, Moskowitz CS, Adsuar R, Wexler LH, et al. Morbidity and mortality after treatment of Ewing sarcoma: A single-institution experience. Pediatr Blood Cancer. 2017. PubMed PMID: 28417551.

14. Hunold A, Weddeling N, Paulussen M, Ranft A, Liebscher C, Jurgens H. Topotecan and cyclophosphamide in patients with refractory or relapsed Ewing tumors. Pediatr Blood Cancer. 2006;47(6):795-800. PubMed PMID: 16411206.

15. Casey DA, Wexler LH, Merchant MS, Chou AJ, Merola PR, Price AP, et al. Irinotecan and temozolomide for Ewing sarcoma: the Memorial Sloan-Kettering experience. Pediatr Blood Cancer. 2009;53(6):1029-34. PubMed PMID: 19637327.

16. Bacci G, Ferrari S, Longhi A, Donati D, De Paolis M, Forni C, et al. Therapy and survival after recurrence of Ewing's tumors: the Rizzoli experience in 195 patients treated with adjuvant and neoadjuvant chemotherapy from 1979 to 1997. Ann Oncol. 2003;14(11):1654-9. PubMed PMID: 14581274.

17. Barker LM, Pendergrass TW, Sanders JE, Hawkins DS. Survival after recurrence of Ewing's sarcoma family of tumors. J Clin Oncol. 2005;23(19):4354-62. PubMed PMID: 15781881.

18. Balamuth NJ, Womer RB. Ewing's sarcoma. Lancet Oncol. 2010;11(2):184-92. PubMed PMID: 20152770.

19. Steffner R. Benign bone tumors. Cancer Treat Res. 2014;162:31-63. PubMed PMID: 25070230.

20. Weatherall PT, Maale GE, Mendelsohn DB, Sherry CS, Erdman WE, Pascoe HR. Chondroblastoma: classic and confusing appearance at MR imaging. Radiology. 1994;190(2):467-74. Epub 1994/02/01. PubMed PMID: 8284401.

21. Douis H, Saifuddin A. The imaging of cartilaginous bone tumours. I. Benign lesions. Skeletal Radiol. 2012;41(10):1195-212. PubMed PMID: 22707094.

22. Schulte M, Brecht-Krauss D, Heymer B, Guhlmann A, Hartwig E, Sarkar MR, et al. Grading of tumors and tumorlike lesions of bone: evaluation by FDG PET. J Nucl Med. 2000;41(10):1695-701. PubMed PMID: 11038000.

23. Chakarun CJ, Forrester DM, Gottsegen CJ, Patel DB, White EA, Matcuk GR, Jr. Giant cell tumor of bone: review, mimics, and new developments in treatment. Radiographics. 2013;33(1):197-211. PubMed PMID: 23322837.

24. Pereira HM, Marchiori E, Severo A. Magnetic resonance imaging aspects of giant-cell tumours of bone. J Med Imaging Radiat Oncol. 2014;58(6):674-8. PubMed PMID: 25256094.

25. Kransdorf MJ, Sweet DE. Aneurysmal bone cyst: concept, controversy, clinical presentation, and imaging. AJR Am J Roentgenol. 1995;164(3):573-80. PubMed PMID: 7863874.

Journal of Radiology Case Reports

www.RadiologyCases.com

FIGURES

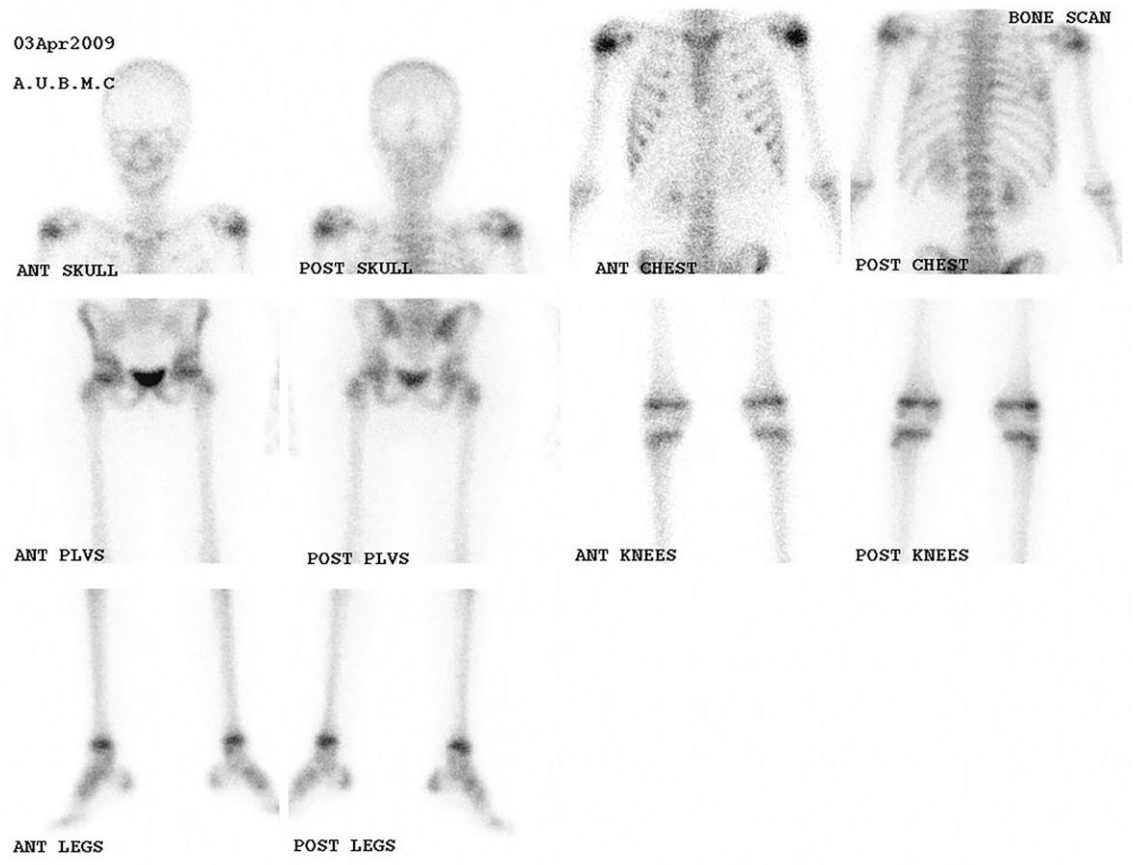

Figure 1: 8-year-old girl with Ewing's sarcoma of the right rib. Bone scan utilizing Tc-99m MDP was performed, demonstrating no abnormal uptake outside the right ribs (site of original tumor), in particular in the left talus.

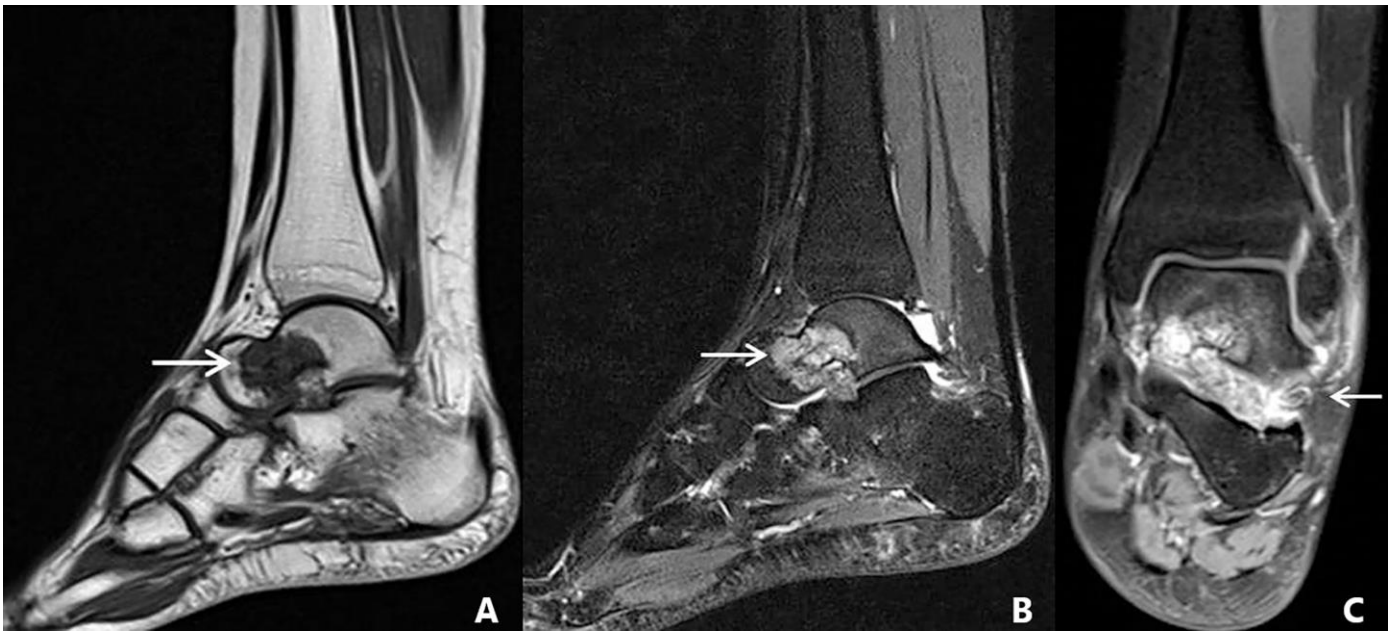

Figure 2: 14-year-old girl with metastatic Ewing's sarcoma to the left talus.
Technique: MRI of the left ankle and foot: (A) sagittal T1-weighted (TR=520, TE=20); (B) sagittal short tau inversion recovery (STIR) (TR=6300, TE=60); (C) coronal T1-fat saturation following IV gadolinium administration (TR=520, TE=20).
Findings: A lesion is seen involving the head and neck of the talus, showing low signal intensity on T1-weighted (arrow) (A), heterogeneous signal with areas of intermediates and high signal intensity on STIR (arrow) (B). A linear hypo-intensity is noted within the lesion in keeping with thick trabeculae. Significant heterogeneous enhancement following IV contrast injection (C). Mild enhancing bone marrow edema is noted around the tumor in (C) with soft tissue edema surrounding the talus and extending into the sinus tarsi (arrow).

Journal of Radiology Case Reports
www.RadiologyCases.com

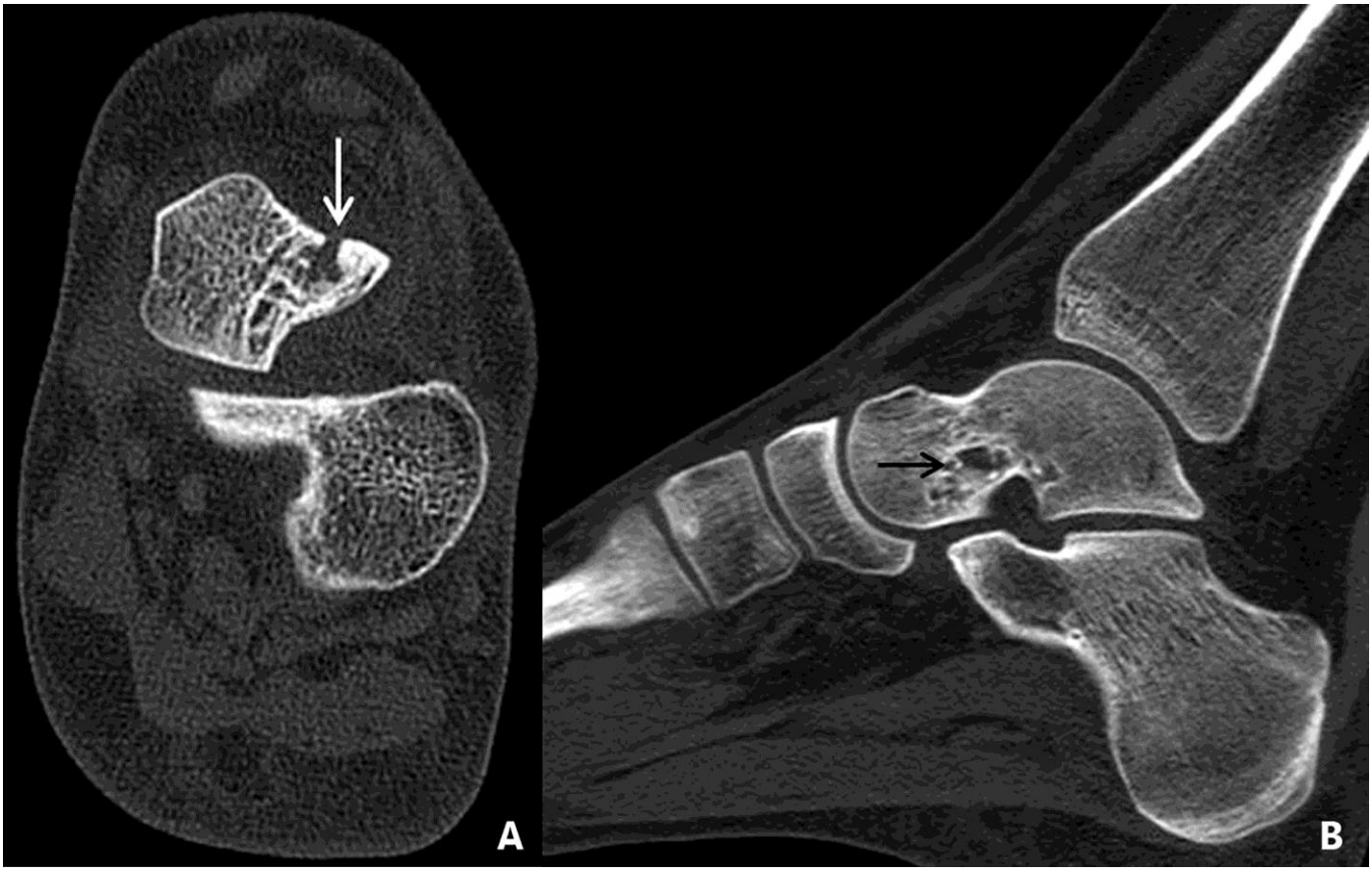

Figure 3: 14-year-old girl with metastatic Ewing's sarcoma to the left talus.
Technique: CT scan of the foot in bone window setting: (A) axial and (B) sagittal reconstruction
Findings: A lytic lesion with thick trabeculae and sclerotic margins is seen in the mid plantar aspect of the talus (black arrow in B). associated with focal cortical disruption along its dorsal aspect (A) (white arrow).

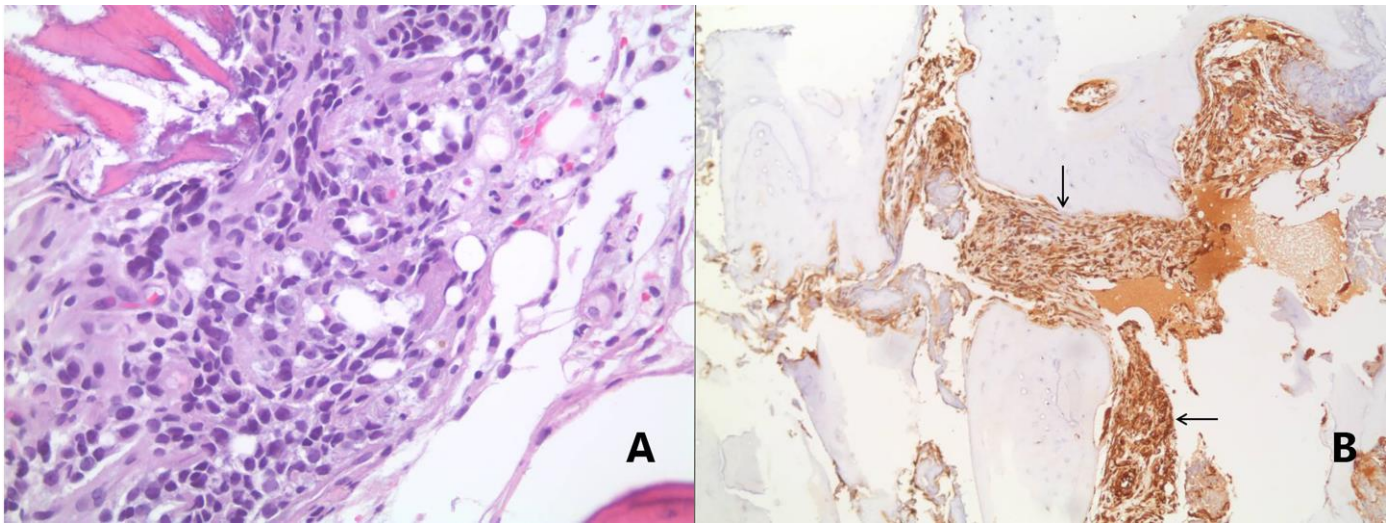

Figure 4: 14-year-old girl with metastatic Ewing's sarcoma to the left talus.
Technique: Pathology: (A) H&E (x40); (B) CD99 immunohistochemistry (x4)
Findings: there is An aggregate of small, round, uniform hyperchromatic cells replacing the bone marrow elements (A), Showing positive staining (arrows) (B).

Journal of Radiology Case Reports
www.RadiologyCases.com

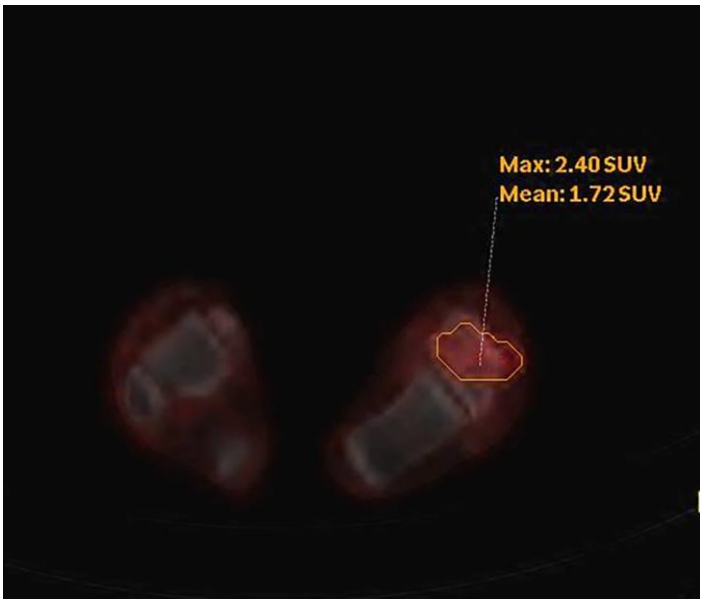

Figure 5 (left): 14-year-old girl with metastatic Ewing's sarcoma to the left talus.
Technique: Axial FDG-PET/CT scan
Findings: Radiotracer uptake is increased within the left talar tumor. SUV measurements are MAX 2.40 SUV, MEAN 1.72 SUV.

Journal of Radiology Case Reports

www.RadiologyCases.com

Etiology	Ewing's sarcoma of the rib with isolated talar bone metastasis
Incidence	Isolated acrometastasis of Ewing sarcoma is extremely rare. Acrometastasis occurs in 0.007-0.3% of all cancer patients
Gender Ratio	No known predilection
Age Predilection	ES occurs in mostly in the second and third decades of life. Metastasis can occur at any point of the disease course.
Risk Factors	Presence of a primary ES lesion. No other known risk factors exist for bone metastasis of ES
Treatment	For ES: Neoadjuvant chemotherapy in conjunction with surgery and/or radiation therapy. Chemotherapy protocol: combination of vincristine, doxorubicin, and cyclophosphamide alternating with ifosfamide and etoposide. For isolated bone metastasis: Chemotherapy (a camptothecin-based regimen) with local control measures i.e. surgery and/or radiation therapy
Prognosis	Single bone metastasis of Ewing's sarcoma portends a five-year survival of 19-30%
Findings on imaging	Acrometastases from Ewing's sarcoma: non-specific and may mimic benign tumor. On CT scan: lytic On MRI: periosteal reaction and a large soft tissue component. T1 signal is low with a heterogeneous enhancement pattern after contrast administration. Mean SUV on FDG PET is typically around 5.3.

Table 1: Summary table of metastatic talar bone lesion from Ewing sarcoma.

Differential	Computed Tomography	Magnetic Resonance Imaging	FDG Positron Emitted Tomography
Chondroblastoma	Lucent lesion with intralesional calcification. Lesions can show marked cortical destruction and a significant periosteal reaction	The T1 signal is low to intermediate Intermediate to high signal on T2 and STIR	Increase uptake
Giant cell tumor	radiolucent lytic lesions with potentially aggressive pattern of cortical destruction, bone loss and periosteal reactions	Low to intermediate T1 signal heterogeneous high and low T2 signal enhancement pattern.	Increased uptake (SUV > 2.0)
Aneurysmal bone cyst	Expansile radiolucent lesion at the metaphysis of long bones. A thin rim with a periosteal reaction.	Variable signal. Fluid-fluid level is typical	No specific findings
Ewing's sarcoma (primary or metastasis)	A lytic lesion with cortical disruption and sclerotic margins	Low T1 signal with a heterogeneous pattern of enhancement	Increased uptake

Table 2: Differential diagnosis and corresponding imaging findings of tarsal bone tumors.

Journal of Radiology Case Reports

www.RadiologyCases.com

ABBREVIATIONS

ABC: Aneurysmal bone cyst
CT: Computed Tomography
ES: Ewing's Sarcoma
FDG: fluorodeoxyglucose
MRI: Magnetic Resonance Imaging
PET: Positron Emission Tomography
STIR: short-tau inversion-recovery

KEYWORDS

Ewing Sarcoma; Talus; Bone metastases; CT scan; MRI; PET-scan

Online access

This publication is online available at:
www.radiologycases.com/index.php/radiologycases/article/view/3164

Peer discussion

Discuss this manuscript in our protected discussion forum at:
www.radiolopolis.com/forums/JRCR

Interactivity

This publication is available as an interactive article with scroll, window/level, magnify and more features.
Available online at www.RadiologyCases.com

Published by EduRad

www.EduRad.org